Annu. Rev. Phys. Chem. 2003. 54:367–96
doi: 10.1146/annurev.physchem.54.011002.103851

First published online as a Review in Advance on February 21, 2003

THEORY OF DIPOLE-BOUND ANIONS

Kenneth D. Jordan and Feng Wang
Department of Chemistry, University of Pittsburgh, Pittsburgh, Pennsylvania 15260, email: jordan@psc.edu, fwang@pitt.edu

Key Words dispersion interactions, solvated electron, Drude model, electron affinity, water cluster

■ **Abstract** The problem of the binding of an excess electron to polar molecules and their clusters has long fascinated researchers. Although excess electrons bound to such species tend to be very extended spatially and to have little spatial overlap with the valence electrons of the neutral molecules, inclusion of electron correlation effects is essential for quantitatively describing the electron binding. The major electron correlation contribution may be viewed as a dispersion interaction between the excess electron and the electrons of the molecule or cluster. Recent work using a one-electron Drude model to describe excess electrons interacting with polar molecules is reviewed.

1. INTRODUCTION

The problem of an electron in the field of a finite fixed dipole comprised of two charges $+Q$ and $-Q$, separated by a distance R has been studied by numerous researchers (1–15). The finite dipole system has an infinity of critical dipole moments for electron binding with an infinite number of bound states appearing at each critical moment. The first three critical moments are 1.6248, 9.6375, and 19.181 D (2, 3). It has also been established that the critical moments remain unchanged if a repulsive term falling off more rapidly with distance from the dipole than does the electrostatic interaction is added (3). These results imply that, in the absence of corrections to the Born-Oppenheimer (BO) approximation (16), "real" molecules with dipole moments greater than 1.625 D must possess dipole-bound anion states. The point-dipole problem has the same critical moments as the finite-dipole problem, however, in the absence of a repulsive core, this problem is unphysical in the sense that binding energies become infinite and the wavefunctions are not normalizable (3, 14, 15).

For molecules or clusters with dipole moments only slightly in excess of the critical value, the electron binding energies associated with dipole-bound anions are very small and corrections to the BO approximation become important. Indeed, Crawford & Garrett (7, 17, 18) have shown that when electronic-rotational coupling is included, the critical dipole moments for binding an excess electron acquire a dependence on the moments of inertia of the molecule, and, as a result, they vary

from molecule to molecule. As a "rule of thumb," real molecules have a first critical dipole moment of about 2.4 D. The other important change resulting from inclusion of corrections to the BO approximation is that the number of bound states is reduced from infinity to a finite number, indeed, only one, unless the dipole is very large (19). This article will deal primarily with species for which the excess electron is sufficiently strongly bound that corrections to the BO approximation are negligible.

The above introductory remarks have focused on the critical dipole moments for electron binding. Equally intriguing is the nature of the interaction between the excess electron and the electrons of the polar molecule or cluster of polar molecules. In a Hartree-Fock treatment, the orbital occupied by a dipole-bound electron is very diffuse and polarized away from the molecule on the positive end of the dipole. As a result, it was long believed that, because of the small overlap between the charge distribution of the excess electron and the electrons of the neutral molecule or cluster, electron correlation effects should play a relatively unimportant role in determining the electron binding energies and other properties of dipole-bound anions (20, 21). However, over the past decade, a rather different picture has emerged, and, it is now known that electron correlation effects can drastically alter the properties of dipole-bound anions (22–29). The main correlation contribution is a dispersion-type interaction between the excess electron and the electrons of the polar molecule of the cluster (22–26). In many cases, fourth- and higher-order correlation effects also make sizable contributions to the electron binding energies. Thus, an accurate description of the dipole-bound anions of these systems using conventional ab initio electron structure methods requires treating electron correlation effects to high order, e.g., by means of the CCSD(T) or CCSDT coupled-cluster methods (30, 31), and using large, flexible basis sets. In light of this, it is of considerable interest that it is possible to develop one-electron models that recover most of the correlation contributions to the electron binding to such species (32–34). This finding, in turn, may suggest new ways of tackling the dispersion problem in general.

Dipole-bound anions were long considered to be rather esoteric, albeit fascinating, entities, without much relevance to mainstream chemistry. However this is no longer the case, as they have been found to be important in a variety of chemical processes. The demonstration that dipole-bound anions can serve as precursors to formation of valence-like anions (35–37) has generated much interest in their role in electron capture in biological molecules such as uracil and thymine (38–43). In addition, many biologically important molecules can exist as zwitterions, which because of their large dipole moments, can form dipole-bound anions (43–47). Dipole-bound anions have also been found to be important in charge-transfer processes. For example, photoexcitation of $I^- \cdot (H_2O)_4$ leads to the charge transfer-complex $I \cdot (H_2O)_4^-$, with the excess electron bound to the cyclic $(H_2O)_4$ cluster, distorted so that it has a large dipole moment (48–53). Dipole-bound anions have also been invoked in explaining diffuse interstellar absorption bands (54).

The recent resurgence of interest in dipole-bound anions and the closely related "solvated-electron" systems has been fueled by important advances on the

experimental front. These advances include the use of Ar-atom vibrational predissociation spectroscopy, enabling one to obtain vibrational spectra of cold anionic clusters (37, 55, 56), femtosecond photodetachment spectroscopy (57), a new generation of experiments using electron transfer from highly excited Rydberg states (58, 59), and improved field ionization methods (60) for estimating the electron binding energies of weakly bound anions.

2. ELECTRON-DIPOLE MODEL

Although the primary focus of the article is on electron correlation effects in electron-polar molecule interactions, it is instructive to first consider the energy levels of an electron bound to a finite fixed dipole. This problem is exactly solvable since the Hamiltonian is the same as that for H_2^+, except for the change of the sign of one of the "nuclei" (61). Figure 1 reports as a function of the dipole moment (μ) the energies of the low-lying levels of this model in the case that the two point charges are $+1$ and -1. In the large dipole limit, the spectrum corresponds to that of the H atom Stark-shifted by a -1 point charge.

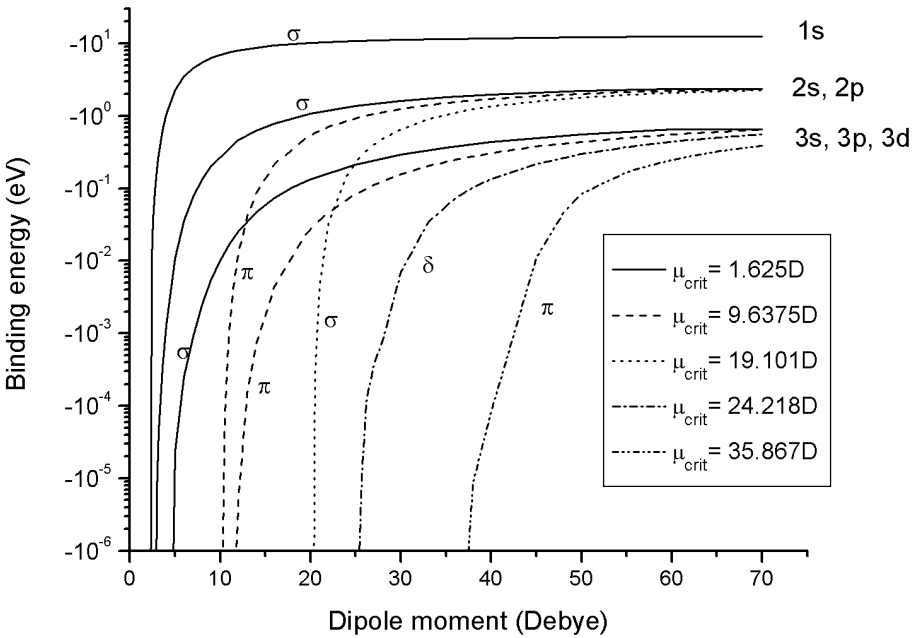

Figure 1 Energies of an electron in the potential due to a finite dipole with $Q = 1$. The energies are calculated using a large set of primitive *s*, *p*, *d*, and *f* Gaussian-type functions centered on the positive charge. Energies less than about 10^{-4} eV in magnitude are unreliable due to the limitations of the basis set.

All of the energy levels associated with the first critical moment ($\mu_1 = 1.625$ D) are σ-like, with the most stable level correlating with the $n = 1$ hydrogenic level in the $R \to \infty$ limit. The higher-lying levels associated with this critical moment correlate with excited states of the H atom, with one level correlating with each of the $n \geq 2$ H-atom levels. All levels associated with the second critical moment of 9.637 D are π-like, with the lowest of these correlating with the $2p\pi$ orbital of the H atom. Finally, the lowest energy level associated with the third critical moment of 19.101 D, correlates with the unfavorably hybridized $2s$-$2p\sigma$ hydrogenic orbital. There is an infinity of larger critical dipole moments, but these are unimportant for most purposes. The reader may note that levels of the same apparent symmetry are shown as crossing in Figure 1. This is not a violation of the noncrossing rule, as the electron finite-dipole problem, like H_2^+, admits an additional constant of the motion (61, 62).

Figure 2 displays the charge distributions of the ground electronic state of the electron-finite-dipole system for four different choices of the parameters: $Q = 1$ and $\mu = 3$ or 6 D (Figure 2*a*), and $Q = 0.5$ and $\mu = 3$ or 6 D (Figure 2*b*).

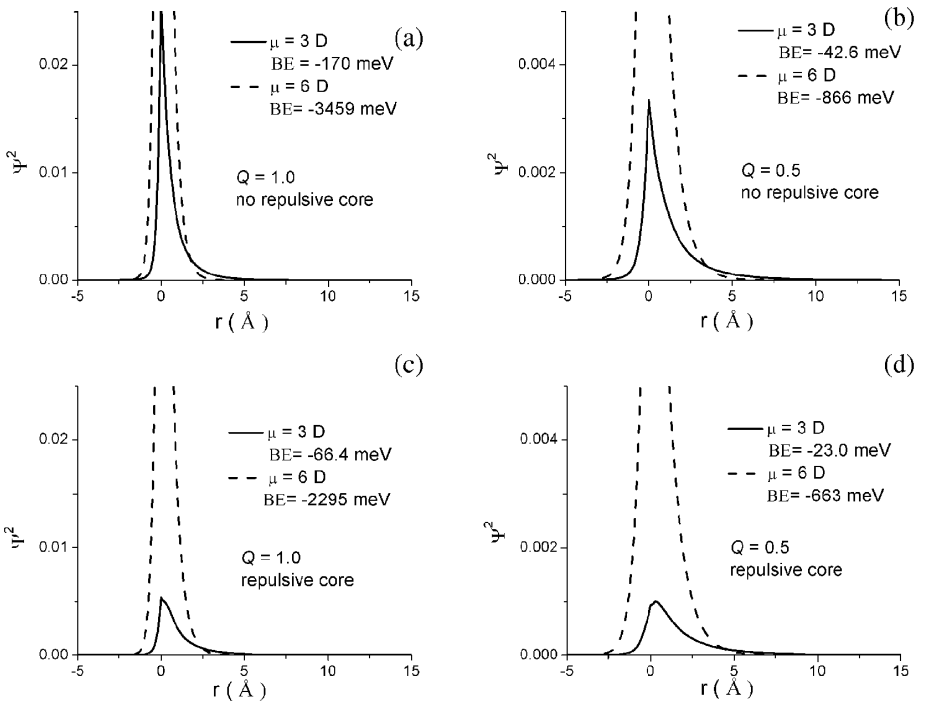

Figure 2 Charge distributions of an excess electron bound to a finite dipole: (*a*) $Q = 1$, $\mu = 3$ and 6 D, no repulsive core, (*b*) $Q = 0.5$, $\mu = 3$ and 6 D, no repulsive core, (*c*) $Q = 1$, $\mu = 3$ and 6 D, repulsive core, and (*d*) $Q = 0.5$, $\mu = 3$ and 6 D, repulsive core. Binding energies are also reported.

From Figures 2*a* and 2*b*, it is seen that the polarization of the wavefunction away from the negative end of the dipole is, as expected, much greater for smaller dipole moments and that the electron density is more localized for the higher charges (keeping the dipole moment fixed).

The most serious shortcoming of the finite dipole model is that it gives electron binding energies much larger than those determined experimentally for real molecules with the same dipole moments. This is primarily a consequence of the neglect of repulsive interactions of the excess electron with the electrons of the neutral molecule. In general, there is appreciable electron density on the atom or atoms constituting the positive end of the dipole, and, as a result, there is an "excluded-volume effect," which reduces electron binding.

This excluded-volume effect can be readily incorporated into one-electron models by adding a repulsive term to the Hamiltonian describing the interaction of the excess electron with the distribution of charges of the neutral molecule (63). Figures 2*c* and 2*d* report the electron charge distributions and binding energies for the four models considered above modified to include a repulsive term centered on the positive end of the dipole. The repulsive core was represented by a single Gaussian function with an exponent of 10 and a prefactor of 1.0, and is roughly comparable to that appropriate for describing binding of an excess electron to HCN (32). As expected, introduction of the repulsive core leads to a decreased electron binding and a more extended charge distribution of the excess electron.

The point-dipole plus repulsive core model is a static model in that it does not allow for relaxation of the core electrons upon the attachment of the excess electron, nor does it allow for correlation interactions between the dipole-bound electron and the core electrons. To include such effects it would appear to be necessary to adopt ab initio methods, treating explicitly all the electrons or at least the valence electrons together with the dipole-bound electron. However, as mentioned in the Introduction, it is, in fact, possible to describe relaxation and the dominant correlation effects within a one-electron model. Before describing one-electron model approaches, we first consider ab initio treatments of dipole-bound anions.

3. AB INITIO TREATMENT OF DIPOLE-BOUND ANIONS

3.1. General Considerations

In discussing ab initio approaches to characterizing dipole-bound anions, it is useful to start with the Koopmans' Theorem (KT) approximation (64) in which the electron affinity (the negative of electron binding energy) is given by

$$EA^{KT} = -\varepsilon_{LUMO}, \qquad 1.$$

where ε_{LUMO} is the energy of the lowest unoccupied molecular orbital obtained from a Hartree-Fock calculation on the neutral molecule. This is a static approximation in that the electron binds in the field of the static potential of the ground state of the neutral molecule or clusters and neither electron relaxation nor correlation

effects are included. The excluded volume effect discussed above is automatically included in ab initio treatments. For molecules or clusters with dipole moments greater than 1.625 D, ε_{LUMO} is necessarily negative, i.e., the LUMO is bound, provided the basis set is sufficiently flexible and the BO approximation is made.

The relaxation contribution to the electron binding can be obtained by carrying out Hartree-Fock calculations on the anion and neutral species, and using the expression

$$\Delta E^{relax} = -EA^{KT} - \left(E^{HF}_{anion} - E^{HF}_{neutral}\right). \qquad 2.$$

Electron correlation contributions to the binding energy can be calculated by a variety of methods, including many-body perturbation theory or coupled-cluster theory. Regardless of the theoretical method employed, it is useful to decompose the EA as follows:

$$EA = EA^{KT} + \Delta E^{relax} + \Delta E^{(2)-disp} + \Delta E^{(2)-nondisp} + \Delta E^{(3)} + \Delta E^{(4)} + \Delta E^{HO}. \qquad 3.$$

In this expression, the second-order correlation correction, $\Delta E^{(2)}$, has been separated into dispersion and nondispersion components (22). $\Delta E^{(3)}$ and $\Delta E^{(4)}$ give, respectively, the third- and fourth-order corrections to the electron binding energy, and ΔE^{HO} collects together fifth- and higher-order corrections. ΔE^{HO} can be estimated, for example, by comparing the EA from MP4(SDTQ) and CCSD(T) calculations.

High-level electronic structure calculations on a variety of dipole-bound anions have revealed that electron correlation effects play a major role in describing the binding of the excess electron in these systems (22–25, 27, 29, 32, 33, 65, 66). This may be seen from examination of Table 1, which summarizes the results of ab

TABLE 1 Contributions to the vertical detachment energy (cm^{-1}) of the dipole-bound anions of selected polar molecules and their clusters as described by ab initio calculations[a]

System	μ_{HF}(D)	μ_{corr}(D)	EA^{KT}	ΔE^{relax}	$\Delta E^{(2)-disp}$	$\Delta E^{(2)-nondisp}$	$\Delta E^{(3)}$	$\Delta E^{(4)}$	ΔE^{HO}	E^{total}	$EA^{expt\ j}$
HCN[–b]	3.29	3.05[h]	11.2	0.4	11.2	–10.9	–0.1	1.2	–0.2	13.2	
$(HCN)_2$[–c]	7.60	6.88[h]	483	49	215	–232	15	17	–17	530	
$(H_2O)_2$[–d]	4.41	4.18[i]	111	7	114	–10	0	20	100	312	363 ± 48[k]
$(HF)_2$[–e]	3.98	3.78[i]	165	14	177	–73	–3	27	81	387	508 ± 24[l,m]
$(HF)_3$[–f]	6.54	6.27[i]	950	104	625	–227	–24	93	145	1666	1613–2420[d]
CH_3CN[–g]	4.34	3.94[i]	53	3	57	–38	4	8	22	108	145–150[n]

[a]The vertical detachment energies are the negatives of the electron binding energies. The second-order dispersion and nondispersion contribution are estimated using a procedure of Gutowski and coworkers. (25, 65) The ΔE^{HO} contributions are obtained by comparing the results of MP4 and CCSDT calculations for HCN and MP4 and CCSD(T) calculations for the other systems.

[b](31); [c] (26); [d] (25); [e] (187); [f](67); [g](188); [h] MP2 dipole; [i] QCISD dipole.

[j] Experimental vertical detachment energies.

[k] (189); [l] A separate experiment (190) gave a VDE of 242 ± 32 for $(HF)_2^-$; [m](191); [n](60).

initio calculations of the vertical electron detachment energies, decomposed along the lines of Equation 3, of HCN^-, $(HCN)_2^-$, $(H_2O)_2^-$, $(HF)_2^-$, $(HF)_3^-$, and CH_3CN^-. Where available, experimental vertical electron detachment energies are included for comparison. Table 1 also reports the dipole moments of the neutral molecules (or clusters) calculated at the Hartree-Fock and correlated [MP2 or QCISD (30)] levels of theory. The calculations have been carried out using flexible Gaussian-type orbital basis sets that are expected to give electron binding energies and dipole moments very close to the complete-basis-set limit values. The second-order contributions to the electron binding energies have been decomposed into dispersion and nondispersion contributions using a procedure of Gutowski et al. (22, 25, 67).

Analysis of the results in Table 1 reveals that, for the molecules and clusters considered, the relaxation contributions to the electron binding energies vary from 4 to 10% of ε^{KT}, whereas, the second-order dispersion contributions are much more important, ranging from 47 to 107% of ε^{KT}. The nondispersion contributions act so as to decrease the electron binding. This is attributed to the fact that for the species considered, electron correlation effects reduce the dipole moment of the neutral molecules (67). As a result, the second-order dispersion and nondispersion contributions to the electron binding energies are of opposite sign, and thus partially cancel. The third-order corrections to the electron binding energies tend to be relatively small, but the fourth- and higher-order corrections are sizable in many cases. Indeed, for $(H_2O)_2^-$, ΔE^{HO} is comparable to the KT binding energy. The origin of the large fourth- and higher-order corrections to the electron binding energies of many dipole-bound anions has proven elusive. We return to this issue later in the review.

In general, good agreement is found between the electron binding energies from CCSD(T) calculations and those measured experimentally, and, in those cases where there are sizable discrepancies [e.g., $(HF)_2^-$ and CH_3CN^-], it is expected that these would be resolved by carrying out CCSDT or multi-reference coupled-cluster calculations. [The CCSD(T) procedure treats triple excitations in a perturbative manner, whereas the CCSDT method treats these excitations nonperturbatively.] The importance of nonperturbative triples for the dipole bound anions of HCN and HNC has been discussed by Peterson & Gutowski (31). The realization that CCSD(T) or CCSDT methods together with large flexible basis sets are required to describe accurately dipole bound anions is disconcerting as such calculations are computationally prohibitive for the large molecule or cluster systems currently being studied experimentally and theoretically (39, 42, 68–70). For these systems, it has often been necessary to compromise on the theoretical method employed.

3.2. Negatively Charged Water Clusters

Electron-water systems have long fascinated researchers. Reactions involving electrons in bulk water are of fundamental importance in radiation chemistry, electrochemistry, and biology (71–75). Yet, even the nature of an excess electron in bulk water remains controversial (76–86). Although the long-held view is that an

excess electron in bulk water is trapped in an approximately spherical cavity (87–90), giving the so-called hydrated electron, Domcke and coworkers have proposed that the excess electron is actually associated with a H_3O species (83). $(H_2O)_n^-$ clusters have also received considerable attention from the experimental and theoretical communities (56, 91–99). There remain several fundamental questions about these species, including the size cluster for which the electron is more stable in an interior rather than a surface state, and how the anions observed experimentally are formed.

$(H_2O)_n^-$ clusters were first detected mass spectroscopically by Haberland and coworkers (100). Figure 3 reproduces a mass spectrum of $(H_2O)_n^-$ clusters from the Johnson group (97). This spectrum is noteworthy by the absence of a peak for the monomer, consistent with its dipole moment being too small to support a dipole-bound anion, and by the occurrence of magic numbers at $n = 2$, 6, 7, and 11, and a monotonically decreasing intensity distribution for $n \geq 15$. The origin of the magic numbers in the $(H_2O)_n^-$ mass spectra is still a matter of debate, although there seems to be a correlation between the dipole moment of the neutral cluster and the intensity of the peak in the mass spectrum, at least for the smaller clusters.

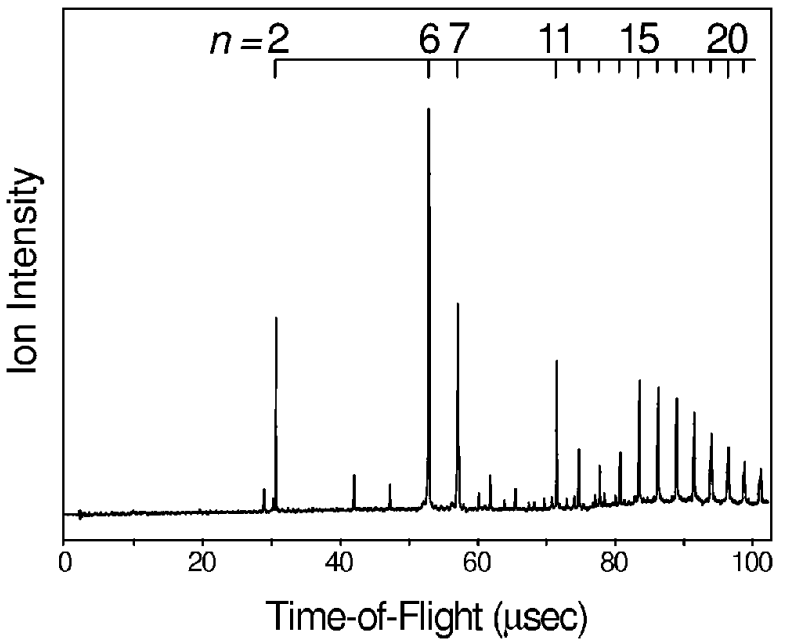

Figure 3 Time-of-flight mass spectrum of $(H_2O)_n^-$ from Reference 97. Note the magic numbers at $n = 2$, 6, 7, and 11. Some of the minor peaks are caused by mixed $(H_2O)_n^- Ar_m$ clusters. In fact, the peaks which appear to correspond to $(H_2O)_4^-$ and $(H_2O)_8^-$ are derived almost entirely from $(H_2O)_2^-$Ar and $(H_2O)_6^-$Ar, respectively.

For example, the most stable forms of the $n = 2, 6, 7$, and 11 clusters, which appear as magic numbers in the anion mass spectrum, have sizable dipole moments (101–103), whereas the most stable isomers of the $(H_2O)_n$, $n = 3$–5, and 8 clusters, for which the corresponding anions are either absent or appear only weakly in the mass spectrum, have zero or small dipole moments. This suggests that the interaction of the excess electron with the dipole field of the neutral clusters may be an important factor in the initial electron capture process. On the other hand, Kim et al. have noted that the $n = 10$ cluster also has a sizable ($\approx$2.7 D) dipole moment but appears only weakly in the mass spectrum, which would appear to contradict the hypothesis that there is a correlation between the dipole moment and anion formation (102, 103). However, it is possible that the low yield of $(H_2O)_{10}^-$ in the mass spectrum is the consequence of a relatively low population of $(H_2O)_{10}$ in the neutral cluster distribution.

The proceeding discussion assumes that the observed $(H_2O)_n^-$ ions result from electron capture by preformed neutral $(H_2O)_n$ clusters. In the experiments of Johnson et al., electrons are ejected into an expansion containing water and Argon, and the Ar-free $(H_2O)_n^-$ clusters are believed to result from electron capture by $(H_2O)_nAr_m$ clusters followed by evaporation of Ar atoms. The most abundant isotope of Ar has a mass close to that of the water dimer, and the weak peaks that appear to correspond to $(H_2O)_4^-$, $(H_2O)_8^-$, and $(H_2O)_9^-$, for the most part, are actually caused by $(H_2O)_2^-Ar$, $(H_2O)_4^-Ar$, and $(H_2O)_7^-Ar$, respectively (97).

Although there is a consensus that the observed forms of $(H_2O)_n^-$, $n = 2$–4, have chain-like structures, the situation regarding the larger clusters is less clear (56, 94, 104–106). Neither the mass spectra nor the measured electron detachment energies allow one to definitely establish the geometrical structures. Recently, the Johnson group has succeeded in measuring vibrational spectra in the OH stretching region for the $(H_2O)_n^-Ar_m$, $n = 5$–9, clusters (55, 56, 107). The presence of attached Ar atoms assures that the clusters are cold ($T \leq 50K$). The comparison of measured spectra with ab initio calculated spectra for various isomers of the bare (i.e., non-Ar solvated) clusters greatly narrows down the possible structures. However, even with the availability of the IR data, the structures of the $(H_2O)_n^-$, $n \geq 5$, clusters remain subject to debate. For example, whereas Ayotte et al. (56) have proposed that the observed IR spectra of $(H_2O)_6^-$ and its deuterium substituted isotopomers are caused by a chain-like isomer, Kim and coworkers have suggested a more three-dimensional structure as the origin of the spectrum (94, 104, 106). One might expect that comparison of the experimental IR spectrum with the calculated spectra for different isomers would permit definitive assignment for a cluster the size of $(H_2O)_6^-$. However, because of the need to employ large, flexible basis sets, it has been necessary to adopt either density functional theory [e.g., Becke3LYP (108–110)] or the MP2 method for calculating the frequencies. Because the Becke3LYP method considerably overbinds the excess electron, whereas the MP2 procedure considerably underbinds it, and because the vibrational frequencies and intensities depend on the degree of localization of the excess electron, neither of these methods can account for the observed IR spectrum in a quantitative manner (56). Density

functional methods, including Becke3LYP, also suffer from the inability to treat long-range dispersion interactions (111). The remedy, namely to calculate the vibrational spectrum at the CCSD(T) level, is too computationally demanding at present. This signals the need for alternative theoretical approaches to treat the anion states of clusters of water and of other polar molecules.

4. ONE-ELECTRON MODEL POTENTIALS APPROACHES TO DIPOLE-BOUND ANIONS

4.1. Drude Model—General Considerations

Although high-level ab initio methods have proven very successful at describing dipole-bound anions, the computational demands of such calculations restrict their applicability to relatively small systems. This limitation greatly hampers the use of ab initio methods for exploring a wide range of structures and calculating the associated vibrational spectra. Hence, it is of considerable interest to develop one-electron models to treating excess electrons interacting with clusters of polar molecules. As is clear from the results reported in Table 1, dispersion-type interactions between an excess electron and the electrons of the neutral molecule or cluster can make a large contribution to the electron binding energies. Although dispersion is inherently a two-electron effect, it can be incorporated into a one-electron model by introducing quantum Drude oscillators on each molecule in the cluster (32).

A Drude oscillator consists of two charges $+q$, and $-q$, coupled harmonically through a force constant k (112). In the absence of an external field, the average displacement between the charges of a Drude oscillator is zero. The quantity q^2/k corresponds to the polarizability (α) of the Drude oscillator, and is generally chosen to match the experimental polarizability of the molecule of interest. Different force constants in the x, y, and z directions can be used to accommodate molecules with highly anisotropic polarizabilities. The Hamiltonian (in atomic units) for the one-electron Drude model is:

$$H_{el} = -\frac{1}{2}\nabla_e^2 + V^{es} + V^{rep} + V^{couple}, \qquad 4.$$

where V^{es} represents the electrostatic interaction between the excess electron and the molecules of the cluster, V^{rep} is a repulsive potential allowing for the "excluded" core region (this term can also include, either implicitly or explicitly, exchange effects), and V^{couple} describes the coupling of the excess electron to the Drude oscillators and is of the form

$$V^{couple} = \frac{q\mathbf{r}\cdot\mathbf{R}}{r^3} f(r), \qquad 5.$$

where $f(r)$ is a damping function that cuts off the unphysical short-range behavior. In our applications, we have used $f(r) = 1 - \exp(-br^2)$, chosen to facilitate integral evaluation over Gaussian-type basis functions.

In solving the resulting one-electron Schrödinger equation, a product basis of the form $|\phi_i(\mathrm{r})\chi_j^{(1)}(\mathrm{R}_1)\chi_k^{(2)}(\mathrm{R}_2)\cdots\rangle$, where ϕ_i is an electron orbital and $\chi_j^{(m)}(\mathrm{R}_m)$ is a harmonic oscillator function associated with the j^{th} energy level of the m^{th} Drude oscillator, is used. In the case of a single Drude oscillator, a second-order perturbation treatment gives rise to polarization and dispersion contributions to the electron binding energy:

$$\varepsilon^{pol} = \frac{q^2}{2k} \sum_{s=x,y,z} \left| \left\langle 0 \middle| \frac{s}{r^3} \middle| 0 \right\rangle \right|^2, \tag{6a.}$$

and

$$\varepsilon^{disp} = -\frac{q^2}{2k} \sum_{s=x,y,z} \sum_{\beta \neq 0} \frac{\left| \left\langle 0 \left| \frac{s}{r^3} \right| \beta \right\rangle \right|^2}{1 - (\varepsilon_0 - \varepsilon_\beta)\sqrt{\frac{m_o}{k}}}, \tag{6b.}$$

where the integration has been carried out over coordinates associated with the Drude oscillator; s denotes the Cartesian coordinates for the electron, and 0 and β refer, respectively, to ground state and excited states of the excess electron (as described by the 0^{th}-order Hamiltonian, which neglects the coupling of the excess electron with the Drude oscillators). A key observation is that the second term in the denominator of Equation 6b, which corresponds to the ratio of the spacings of the energy levels of the excess electron to those of the Drude oscillator, is much smaller than one, so that the dispersion contribution is relatively insensitive to the choice of k or m_o, the mass associated with the Drude oscillator. In the applications, presented below, q is chosen to be 1, m_o is taken to be the mass of an electron, and k is chosen so that q^2/k gives the experimental polarizability for the monomer of interest.

Equation 6b may be approximated as

$$\varepsilon^{disp} \approx \frac{q^2}{2k} \frac{\overline{\varepsilon}}{\overline{r}^6} \sum_{s=x,y,z} \sum_{\beta \neq 0} \frac{|\langle 0 | s | \beta \rangle|^2}{(\varepsilon_0 - \varepsilon_\beta)}, \tag{6c.}$$

which is a London-type expression involving a product of the polarizabilities of the Drude oscillator and the excess electron, $\overline{r}$ is an effective average distance of the excess electron from the oscillator, and $\overline{\varepsilon}$ is the mean excitation energy of the excess electron. This makes clear that the large dispersion energies of dipole-bound anions may be thought of as arising from the very large polarizability of the weakly bound excess electron. (This is also the case for solvated-electron species, discussed below.) A unique aspect of dipole-bound (and solvated-electron) anions is that the polarizability of the weakly bound electron derives entirely or almost entirely from excitations into the continuum, which, in the approach described above, has been discretized by the use of the Gaussian-type basis set.

For the problem of an excess electron interacting with a cluster of polar molecules, a Drude oscillator is located on each monomer, and the second-order expressions for polarization and dispersion involve sums over the contribution from each oscillator. (For large molecules, the approach can be extended to employ multiple

Drude oscillators on individual molecules.) The coupling between Drude oscillators located on different monomers in a cluster accounts for intermolecular induction and dispersion (113). The former is crucial for obtaining the correct overall charge distribution, in particular, the dipole moment, for the cluster of interest. In our applications of the Drude oscillator approach to electron binding to HCN and H_2O clusters, the Hamiltonian has been partitioned so that the intermolecular induction is incorporated into the zeroth-order Hamiltonian for the excess electron (32).

In principle, third- and higher-order correlation effects between the excess electron and the Drude oscillators can be treated with any of the standard approaches from electronic structure theory, including many-body perturbation theory, coupled-cluster theory, diffusion Monte Carlo, or configuration interaction (CI). Our applications have used the CI approach, with the restriction that only terms involving at most double excitations are retained.

Models for including dispersion interactions between an excess electron and a cluster of polar molecules have been introduced by two groups. The Drude-model approach presented above was introduced by our group. Sindelka et al. (34) have also recently introduced a model for calculating second-order dispersion interactions between an excess electron and a polar molecule or cluster of polar molecules. The main difference is that whereas Equation 6a employs a discretization of the continuum, Sindelka et al. calculated the dispersion energy by doing an integral over the continuum. A second difference is that we have damped the short-range coupling between the electron and the polarizable monomers, while Sindelka et al. used an undamped interaction. However, this damping is relatively unimportant for the second-order energies. The two approaches also differ in terms of the choice of excitation energy associated with the monomer. However, as argued above, the dispersion energy is relatively insensitively to the monomer excitation energy.

4.2. Applications of the Drude Model to Water Clusters

We now consider in more detail the use of one-electron model potentials for describing the interaction of an excess electron with water. Water has been chosen as the focus because of the large body of experimental and theoretical work done on excess electrons interacting with water in clusters, films, and bulk, and because there are several unresolved issues concerning electron-water systems that cannot be answered by current ab initio methods.

There is a rich history of one-electron model approaches to treating electron-water systems. In particular, we note the pioneering work of Landman and coworkers (114), Rossky et al. (115), Staib & Borgis (116), and Berne and coworkers (92). The key features of the models introduced by these researchers, as well as of a more recent model of Mosyak et al. (117), are summarized in Table 2. These models have been used to address a variety of problems, including estimating the size water cluster for which it is more favorable for an excess electron to be bound in the interior as opposed to the surface (118–120), calculating electron transport through water films (121), and simulating the dynamics of the solvated electron following photoexcitation (122, 123). Most of these one-electron models allow

TABLE 2 Characteristics of various one-electron models for describing negatively charged clusters of water molecules or an excess electron in bulk water

Potential	Water-water[a,b]	Electron-water
Schnitker-Rossky (115)	SPC (192), rigid, nonpolarizable, $\mu = 2.27$ D	2-body polarizable,[c] $-\frac{\alpha}{2r^4}\left[1 - e^{-(r/r_c)^6}\right]$
Barrett-Landman (114)	RWK2-M (193), flexible, nonpolarizable, $\mu = 1.87$ D	2-body polarizable, $-\frac{1}{2}\frac{\alpha}{\left[\left\vert\vec{r} - \vec{R}_j\right\vert^2 + R_c^2\right]^2}$
Staib-Borgis (116)	pTIP4P (194), rigid, polarizable via fluctuating charge, $\mu = 1.85$ D	fluctuating charge, self-consistent polarizable
Wallqvist-Berne (92)	modified central force potential (195), flexible, nonpolarizable, $\mu = 1.86$ D	2-body polarizable, $-\frac{\alpha}{2r^4}\left[1 - e^{-(r/r_c)^{12}}\right]$
Mosyak et al. (117)	pfSPC (117, 196), flexible, polarizable,[c] $\mu = 2.02$ D	self-consistent polarizable,[d] $-\frac{1}{2}\sum \mu_j \cdot E_j$, with $-\frac{1}{2}\frac{\alpha}{\left[\left\vert\vec{r} - \vec{R}_j\right\vert^2 + R_c^2\right]^2}$
Wang-Jordan (33)	Dang-Chang (124), rigid, polarizable, $\mu = 1.85$ D	self-consistent polarization and dispersion via Drude oscillators[e]

[a]Models with fixed monomer geometries are designated as rigid, and those in which the monomer geometries can relax are designated as flexible.

[b]The dipole moments are for the isolated monomers.

[c]Two-body polarizable models allow the excess electron to polarize the water molecules (with polarizability centered on O), but neglect couplings between the induced dipoles. Models designated as self-consistent polarizable treat electron-water and water-water polarization self-consistently.

[d]The polarizable water model of Mosyak et al. introduces a polarizable site with polarizability $\alpha = 1.44$ Å^3 at the position of the O atom.

[e]The polarizable center is on the *M* site, which is on the C_2 axis, 0.215 Å from the oxygen atom, displaced toward the H atoms (33).

for polarization of the water molecules by the excess electron, but none allow for dispersion interactions between the excess electron and the water molecules. As is clear from Table 1, the dispersion contribution to the electron binding energy is typically an order of magnitude more important than polarization (at least for small clusters) and it is generally comparable to the electrostatic binding energies. This raises the possibility that dispersion interactions could significantly affect the dynamics of solvated electrons or impact the preference for electron binding in the interior versus the surface of a cluster.

The Drude model described in Section 4.1 permits inclusion of dispersion interactions between an excess electron and clusters of polar molecules, and has recently been applied to water clusters (33). For treating the water-water

interactions, we have adopted the Dang-Chang (DC) water model (124), which has been found to provide a good description of neutral water clusters (124, 125). This model is based on a rigid monomer, with the geometry chosen to reproduce that of the gas-phase water molecule. Positive point charges (0.519) are located on the H atoms, and a negative point charge (−1.038) is located at the position *M*, which is on the rotation axis, displaced 0.215 Å from the O atom, toward the H atoms. The DC charge distribution closely reproduces the experimental dipole and quadrupole moments of the water monomer (126, 127). The DC model also employs a single isotropic polarizable center, located at the *M* site, with α chosen to reproduce the experimental polarizability (128). Finally, it includes Lennard-Jones interactions between O atoms of different monomers.

In modifying the DC water model for describing electron binding to water clusters, the polarizable *M* site was replaced with a Drude oscillator at the same location and with the same polarizability (q^2/k). Since many-body dispersion effects are expected to be relatively small in $(H_2O)_n^-$ clusters, the intermonomer dispersion was actually described by means of the R^{-6} Lennard-Jones terms in the DC model rather than via interactions between the Drude oscillators. In other words, it was assumed that three-body dispersion effects involving the excess electron and two water monomers are relatively unimportant. The key features of the resulting Drude model for water are summarized in Table 2.

The final steps in developing the DC-based Drude model for water involved choosing a suitable repulsive potential and determining an appropriate *b* cutoff parameter for the coupling term. The repulsive potential was determined from Hartree-Fock calculations on H_2O at the DC geometry and using a procedure developed by Schnitker & Rossky (115). The repulsive potential was represented as a superposition of *s*, *p*, and *d* Gaussian functions on the three atom sites of the DC model and was scaled so that the one-electron model potential, with the charges and polarizability being chosen from Hartree-Fock calculations rather than from the DC model, gave for $(H_2O)_2$ the same value of the KT electron binding energy as obtained from ab initio Hartree-Fock calculations. After determination of the repulsive potential, the charges and polarizability were reset to the DC values. The *b* cutoff parameter was then chosen so that the electron binding energy of $(H_2O)_2$ obtained from the Drude-model CI calculations matches that from ab initio CCSD(T) calculations. These calculations used the geometry of $(H_2O)_2^-$ obtained from ab initio MP2 optimizations with the constraint of rigid monomers (see Figure 4).

One of the major challenges in describing excess electrons bound in nonvalence orbitals of clusters of polar molecules is the choice of a suitable basis set. This problem exists for both ab initio and one-electron model potential calculations. Many of the issues connected with choosing basis sets for treating dipole-bound and solvated electron species are covered in a recent paper by Skurski et al. (129). Here we briefly describe some of the problems inherent in choosing Gaussian-type basis sets to represent the excess electron as described by a one-electron model.

In some cases, e.g., for the chain form of $(H_2O)_3^-$ or $(H_2O)_4^-$, it suffices to employ an expansion of diffuse *s* and *p* functions centered on the oxygen atom

of the terminal water at the positive end of the dipole. However, for certain other geometries, or for mapping out geometrical rearrangement pathways, it is not obvious where the diffuse functions should be centered. In principle, a single-center expansion should suffice for these cases as well. However, to properly describe the electronic wavefunctions for arbitrary geometrical arrangements, this approach requires the inclusion of very high angular momentum functions, making the calculations computationally prohibitive. The alternative approach of locating a large set of *s* and *p* functions on each monomer is also computationally expensive and is prone to linear dependency. A comprise, which works well for many systems, is to employ a large single-center expansion of diffuse *s* and *p* functions in conjunction with smaller sets of *s* and *p* functions centered on each monomer. This approach, together with optimization of the location of the center of the large expansion of diffuse functions, has been used in ab initio calculations of rearrangement pathways of $(H_2O)_3^-$ and $(H_2O)_4^-$ (33, 130).

In the Drude-model calculations on the water dimer and on the larger water clusters discussed below, the electronic orbitals were expanded in a basis set of Gaussian-type functions, with two *s* and one *p* functions on each *H* atom and with a large set of diffuse *s* and *p* functions on a "floating" center, the position of which was optimized in an earlier ab initio study (130). The inclusion of the functions on the H atoms obviates the need to include high angular momentum functions on the floating center. The Drude model should be well suited for use with plane-wave basis sets or with grid-based or path integral approaches to describing the excess electron.

The one-electron Drude model for electron/water systems has been tested on the crown and chain-like forms of $(H_2O)_3^-$ and $(H_2O)_4^-$ (see Figure 5) (33), by comparing the electron binding energies obtained with the Drude model with those from ab initio calculations (M. Gutowski, personal communication). The crown-like structures are assumed to have C_3 and C_4 symmetry in the case of $(H_2O)_3^-$ and $(H_2O)_4^-$, respectively. As seen from the results in Table 3, the CI calculations using the Drude model give electron binding energies for the $(H_2O)_3^-$ and $(H_2O)_4^-$ clusters nearly identical to the ab initio CCSD(T) values. The electron binding energies, from both the Drude model and the ab initio calculations, are enhanced by a factor of two to four by the inclusion of correlation effects, with a significant portion of the enhancement being caused by third- and higher-order correlation effects. This leads naturally to the question as to how the electronic charge distributions of these clusters are modified by the inclusion of the correlation effects. This issue is addressed in Figure 6, which displays the distributions of an excess electron bound to the crown- and chain-like forms of $(H_2O)_4$. The wavefunctions used to generate these plots were obtained from the Drude model calculations. The charge distributions associated with the KT and MP2 wavefunctions are essentially identical. This is an expected result because dispersion interactions do not generally cause large changes in charge distributions. On the other hand, there is a sizable contraction in the charge distributions upon inclusion of the fourth- and higher-order correlation effects. An analysis of the CI wavefunction reveals that the contraction is caused by configurations in which the excess electron is excited but the Drude oscillators are unexcited. The origin of the importance of these single

TABLE 3 Electron binding energies (meV) for the linear and crown forms of $(H_2O)_3^-$ and $(H_2O)_4^-$ calculated using the one-electron Drude model and all-electron ab initio methods[a]

		Binding energy		
Species	**Method**	**KT**	**MP2**	**CCSD(T)/CI[b]**
Crown $(H_2O)_3^-$	ab initio	3.3	5.7	13.0
	Drude model[c]	3.3	7.3	13.6
Linear $(H_2O)_3^-$	ab initio	60.7	97.1	127.0
	Drude model[c]	60.4	105.3	128.6
Crown $(H_2O)_4^-$	ab initio	12.5	20.9	36.5
	Drude model[c]	12.9	25.6	40.0
Linear $(H_2O)_4^-$	ab initio	110.2	170.3	209.6
	Drude model[c]	109.2	179.9	212.5

[a]All results obtained at ab initio MP2–optimized geometries under the constraint of rigid monomers, to facilitate comparison of the model potential and ab initio results. The monomer OH bond lengths and HOH angle are fixed at the experimental values.

[b]The ab initio and model potential results are from CCSD(T) and CI calculations, respectively.

[c]In the Drude model calculations, the KT energies are obtained using Hartree–Fock charges, and the MP2 and CI energies are obtained using the DC charges.

excitations is readily seen from a perturbation theoretical analysis, which reveals that the associated denominators involve factors of the form $\epsilon_0 - \epsilon_j$, where ϵ_0 and ϵ_j are the energies of the excess electron (in the absence of coupling to the Drude oscillator) in the ground and excited states, respectively. These energy gaps can be quite small, given the weak binding of the excess electron. Although this analysis was based on the results of calculations using the one-electron Drude model, we expect that the main conclusion, namely, that single excitations cause sizable contraction of the charge distributions of excess electrons bound to water and other polar molecule clusters, to hold also for ab initio calculations on these species. The importance of single excitations for the electron binding energies of dipole bound anions as treated by ab initio methods has been noted by Gutowski et al. (23). One important difference between the Drude model and standard ab initio treatments is that in the former, the excess electron "sees" a "realistic" charge distribution at

Figure 6 Distributions of an excess electron bound to crown (*a*) and linear (*b*) forms of $(H_2O)_4^-$. Results obtained using the one-electron Drude model. In (*a*), the charge density is plotted along the line perpendicular to the plane of four O atoms, with the origin taken to be the center of this plane. The $+r$ direction is toward the "up" H atoms. In (*b*) the charge density is plotted along the dipole axis with the origin taken to be the O atom of the terminal acceptor water molecule. The $+r$ direction is away from the chain. (Reproduced from Reference 33 with permission.)

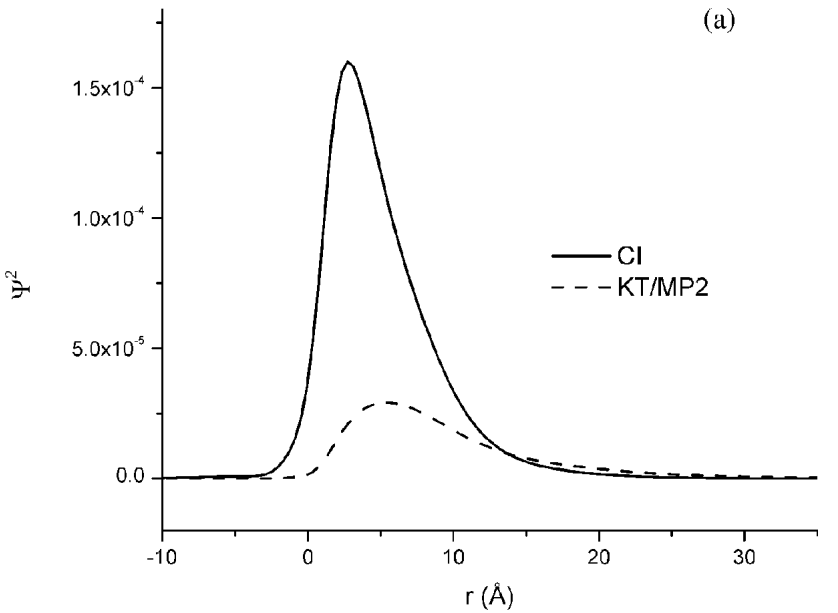
(a)
1.5x10-4
1.0x10-4
5.0x10-5
0.0
Ψ2
CI
KT/MP2
-10
0
10
20
30
r (Å)

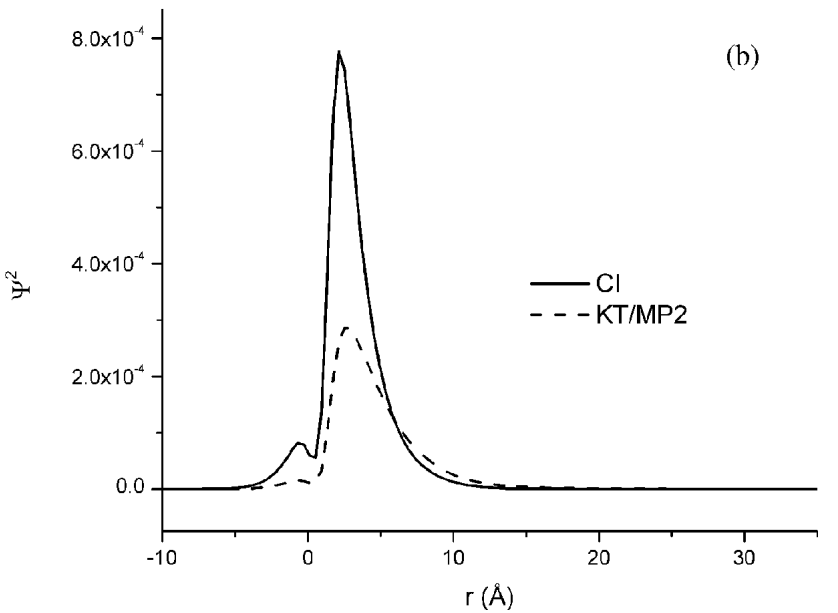
(b)
8.0x10-4
6.0x10-4
4.0x10-4
2.0x10-4
0.0
Ψ2
CI
KT/MP2
-10
0
10
20
30
r (Å)

zeroth order, whereas in ab initio calculations it "sees" the Hartree-Fock charge distribution of the neutral molecule or cluster at zeroth order. Consequently, ab initio calculations starting from Hartree-Fock wavefunctions necessarily include at second- and higher-order corrections associated with "renormalization" of the charge distribution of the neutral species.

The Drude model is also well suited for describing electron binding to mixed clusters containing polar molecules and other atoms or molecules that do not have low-lying valence-type anion states. For example, the Drude model has recently been applied to $(H_2O)_2^- Ar_m$, $m \leq 12$, clusters, again, using a one-electron Hamiltonian, but with polarization and dispersion interactions involving the Ar atoms as well as the water molecules being described by Drude oscillators (B. Tsai, K.D. Jordan, personal communication). These calculations reveal that the variation in the electron binding energies caused by the clustering with Ar atoms is the result of an interplay of several factors, including changed electrostatics resulting from the induced dipoles on the Ar atoms, an "excluded-volume" effect caused by the repulsive potential on the Ar atoms, and polarization and dispersion interactions between the excess electron and the Ar atoms. They also reveal that if there are solvent atoms or molecules occupying the region of space that would be occupied by the excess electron in the absence of the solvent, then the binding energy may become so small that the excess electron would not remain bound if corrections to the BO approximation were included even though the dipole moment is larger than 2.4 D.

5. USE OF THE DESIGNATION "DIPOLE-BOUND"

In recent years there has been a tendency to reserve the term dipole-bound anion for species in which the electron binding energy is relatively weak, e.g., less than 0.1 eV (133, 134). According to such a criterion, the ground state anions of the chain form of $(H_2O)_6$ and of NaCl, for example, would not be classified as dipole-bound. Although the excess electron is bound by over 0.4 eV in these species (97, 135, 136), most of its charge density is still outside of the valence region of the neutral molecule or cluster. Also the one-electron Drude-type model is as successful at describing binding of excess electrons to $(H_2O)_6$ and NaCl as to species such as CH_3CN and $(H_2O)_2$, which display much weaker electron binding. For these reasons, we believe that it is also appropriate to refer to these more strongly bound anions as dipole-bound.

It is interesting to consider the application of the one-electron Drude model to ionic species, using NaCl as the example. There are two ways of setting up a Drude model for describing an excess electron interacting with NaCl: 1. choosing atomic charges that reproduce the experimental dipole moment and employing a single polarizable site with the polarizability chosen to reproduce the experimental molecular polarizability, or 2. employing charges of $+1$ and -1 on the Na, and Cl, respectively, and introducing Drude sites on each ion and allowing polarization

of each Drude oscillator by the other ion. (Because Na^+ is much less polarizable than Cl^-, to a good approximation, only a single Drude oscillator, located on the Cl^- ion, need be employed.) In the second approach, it is necessary to damp the interactions of the ions with the Drude oscillators to obtain a correct value of the induced dipole moment. For ionic species such as NaCl, in contrast to the nonionic species discussed above, the polarization and dispersion contributions to the electron binding energy are comparable in magnitude and are small compared with the electrostatic contribution to the binding of the excess electron. This is a consequence of the more highly localized excess electron in NaCl compared with the more weakly bound anions discussed above.

6. "SOLVATED-ELECTRON" AND RELATED SYSTEMS

Arrangements of polar molecules with small, or even zero, net dipole moments can bind excess electrons (40, 137, 138). Geometries with the positive ends of the monomer dipoles pointing toward one another and with the excess electron "trapped" in the resulting attractive potential in the interior of the cluster are often referred to as solvated-electron species. The hydrated electron (86, 88, 90) is probably the most famous solvated-electron species. (Here we have assumed that the commonly accepted picture of the hydrated electron—in which the electron is bound in an approximately spherical cavity surrounded by water molecules with "free" OH groups pointing toward the center of the cavity—is correct. Recent theoretical studies have demonstrated that dimers of various biomolecules such as urea can also form solvated-electron anions (139).

To illustrate the properties of solvated-electron species, we consider the $(HF)_n^-$, $n = 2$–6 clusters, with the molecules arranged so that the net dipoles are zero. These species have been examined in detail by Gutowski and coworkers (67, 137), and the geometrical arrangements of the first three members of this species are shown in Figure 7. Although these structures are obviously unstable for the neutral molecules, the resulting anions are stable in the sense that they lie energetically below the neutral clusters at the same geometry arrangement. There are other geometrical arrangements of the $(HF)_n^-$ clusters that are intermediate between dipole-bound and symmetric solvated-electron in nature. The asymmetrically solvated species are typically more stable than the fully symmetric solvated species (137). There is experimental evidence for an asymmetrically solvated form of $(HF)_3^-$ (137).

Table 4 summarizes the contributions, obtained from ab initio calculations, of various terms to the electron binding energies for $(HF)_n^-$, $n = 2$–6, solvated-electron species. In each case, the results are reported at the geometry for which the anion, constrained to the symmetry indicated in the Table and described by MP2 calculations, has its potential energy minimum. From comparison of the results in this Table with those in Table 1, it is seen that the dispersion contributions to the electron binding energies are even more important for the solvated-electron

TABLE 4 Electron binding energies (meV) of the $(HF)_n$, $n = 2$–6, solvated–electron species[a,b]

Species	Symm.	EA^{KT}	ΔE^{relax}	$\Delta E^{(2)-disp}$	$\Delta E^{(2)-nondisp}$	$\Delta E^{(3)}$	$\Delta E^{(4+HO)}$	EA^{total}
$(HF)_2$	$D_{\infty h}$	12.3	3.5	42.0	–16.7	–0.5	12.8	53.4
$(HF)_3$	D_{3h}	243.8	158.9	427.1	–211.6	–17.4	32.1	632.9
$(HF)_4$	T_d	807.9	404.4	685.4	–427.3	–26.1	32.2	1476.5
$(HF)_5$	D_{3h}	1357.9	497.3	753.6	–513.1	–21.8	26.0	2099.9
$(HF)_6$	O_h	1930.7	556.2	796.6	–584.1	–18.0	9.8	2691.2

[a] $(HF)_2$ and $(HF)_3$ results from Reference 67.

[b] $(HF)_4$, $(HF)_5$, and $(HF)_6$ results from M. Gutowski, personal communication.

systems than for the corresponding dipole-bound anions. For example, for $(HF)_3^-$, the second-order dispersion contribution to the electron binding energy is 427 meV for the solvated-electron species but only 77 meV for the corresponding dipole-bound anion. In part, this is a consequence of the strong dependence of the dispersion interaction between the excess electron and a particular monomer on the distance of the monomer from the excess electron. (See Equation 6c.) In chain-like isomers, the dispersion contribution to the electron binding is greatest for the terminal monomer closest to the excess electron, and falls off rapidly, along the chain.

Skurski et al. (140, 141) have also considered species with two dipoles oriented as shown in Figure 8*a*, which also have zero net dipole moments. These authors have referred to electrons bound to this charge arrangement as "bi-dipole" bound. Molecules or clusters with charge arrangements such as those shown in Figures 8*b* and 8*c*, also have zero net dipole moments and may bind an excess electron to give a so-called quadrupole-bound anion (59, 142–146). The ground state of $(BeO)_2$ anion with a D_{2h} geometry is an example of a quadrupole-bound anion (143, 144). Although one can refer to $(BeO)_2^-$ as quadrupole bound, such species do not have a critical quadrupole moment analogous to the critical dipole moment for electron binding in dipole fields (142, 145, 146). It has been proposed that formamide dimer, p-dinitrobenzene, and even CS_2 form quadrupole-bound anions (36, 147–149). However, we are unaware of any conclusive ab initio calculations that demonstrate quadrupole bound anions for these species.

The solvated-electron, bi-dipole-bound and quadrupole-bound anion species are closely related in that the binding of an excess electron in each case (as well as in dipole-bound anions) results from the existence of a highly attractive electrostatic potential over a sufficiently large region of space. If the highly attractive region does not "span" a large region of space, then by consequence of the uncertainty principle, "confinement" of the electron is accompanied by a large increase in the kinetic energy causing it to become unbound. For this reason, the solvated-electron form of $(HF)_2^-$ becomes unstable to electron detachment when the H atoms of the two HF molecules are brought to a separation of about 5.2 Å.

7. DIPOLE-BOUND VERSUS VALENCE-TYPE ANION STATES

Thus far, the discussion has focused on species for which there are no bound or low-lying unbound (temporary) (150) valence-type anion states. In recent years there has been considerable interest in molecules that possess both a dipole-bound anion and one or more low-lying valence-type anion states (35, 36, 39, 41, 42, 151, 152). Classic examples are H_2CHO, H_2CCC, and H_2CCN (24, 153, 154). Two systems that have attracted recent attention are nitromethane and uracil, which have dipole moments of 3.46 and 4.6 D, respectively (155).

In considering nitromethane and its low-lying anion states, the key coordinate is the tilting angle, θ, between the plane of the NO_2 group and the C-N bond. This angle is about 1.5° for the ground state of the neutral molecule and about 34° for the ground state π^* valence anion (156). At the equilibrium geometry of the ground state of the neutral molecule, the π^* anion lies energetically 450 meV above the neutral and the dipole-bound anion state energetically 12 meV below the neutral (157). On the other hand, the valence anion at its optimized geometry is calculated to lie 260 meV below the neutral molecule (35). As a result, the dipole-bound anion can act as a "doorway" state for formation of the valence-type anion (27, 35, 37, 156, 158–160). Because of the coupling to the underlying valence state, a pure dipole-bound anion state is not expected to exist on a μs timescale (158). The dipole-bound to valence-bound pathway is further facilitated by attachment of cold Ar atoms (37). One can also envision starting with the valence anion and using photoexcitation to probe the dipole-bound anion. In case of nitromethane, vertical excitation from the valence anion would produce the dipole-bound state highly vibrationally excited in the NO_2 "wag" vibration, which would be expected to cause rapid electron autodetachment.

The uracil molecule has a π^* valence-type temporary anion state lying energetically (in a vertical sense) about 0.22 eV above the ground state of the neutral molecule (161, 162). In general, valence-type anions tend to be more stabilized by solvent atoms or molecules than are dipole-bound anions. In fact, solvent atoms or molecules may destabilize a dipole-bound anion because of an excluded-volume effect, "pushing" the anion above the neutral molecule and causing it to become unstable to electron detachment. In the case of uracil, complexation with just a single water molecule reverses the relative stability of the dipole-bound and valence-type anion states (69, 162, 163). This has been demonstrated by comparison of the photoelectron spectra of the uracil$^-$ and uracil$^- \cdot (H_2O)$ ions. Various researchers have raised the possibility that dipole-bound anions could act as doorway states for electron capture by biomolecules in biological media (44, 159, 160). However, it is possible that the fully solvated molecules will not possess dipole-bound anions (164).

In systems such as nitromethane and uracil in which both dipole-bound and valence-type anions occur very close in energy (and, in fact, can mix if symmetry permits), one-electron models are not adequate and ab initio electronic

structure methods are required to correctly describe the various anion states of interest.

8. REARRANGEMENTS OF DIPOLE-BOUND ANIONS

Most of the theoretical work on dipole-bound anions and solvated-electron species has focused on local minima, and surprisingly little theoretical work has been done on rearrangement pathways between the local minima. One of the unique aspects of this problem is that electron autoionization can become important if the potential energy surface of the anion crosses that of the neutral cluster along the rearrangement pathway. Obviously, if electron autoionization is sufficiently fast then the isomerization will not occur. Alfonso & Jordan have calculated, at the MP2 level, rearrangement pathways between the crown-like and chain-like forms of $(H_2O)_3^-$ and $(H_2O)_4^-$ (130). For these pathways, the dipole moment is always sufficiently large that the anion state is dipole-bound and thus lies energetically below the neutral cluster (at the same geometry). On the other hand, the $HCN^- \rightarrow HNC^-$ rearrangement is subject to electron detachment because the dipole moment of the neutral molecule drops as low as 1.31 D along the reaction pathway. A similar example is the rearrangement between the amino and the imino forms of 9-acridinamine. The amino form of 9-acridinamine has a dipole moment of 3.2 D, whereas the imino form has a dipole moment of 3.8 D (165). However, the direction of the dipole moment inverts during the tautomerization process (Figure 9), and, as a result, electron detachment should be important (165, 166). Species such as $(HF)_2^-$ can also undergo rearrangements via double tunneling (167), which may permit isomerization even in those cases that the transition state structure is subject to rapid electron autoionization.

9. DIPOLE-BOUND DIANIONS

Recently, Skurski and coworkers (168) have examined the problem of the binding of two electrons in a dipole field of a neutral molecule. These authors have shown that in the point-dipole limit, the critical dipole moment for binding two electrons is the same as that for binding one, namely, 1.625 D. However, for finite dipoles, the situation is quite different, namely, for a finite dipole comprised of two charges $+Q$ and $-Q$, the second electron does not bind if $Q \leq 0.91e$, regardless of the magnitude of the dipole (146, 168–170). Skurski et al. (171) have demonstrated computationally the existence of dipole-bound dianions of novel molecules with positively charged Ca ions and negatively charged superhalogen groups. At present, there is no unambiguous experimental evidence of dipole-bound dianions, except the trivial case of two independent dipole-bound anions separated by a large distance.

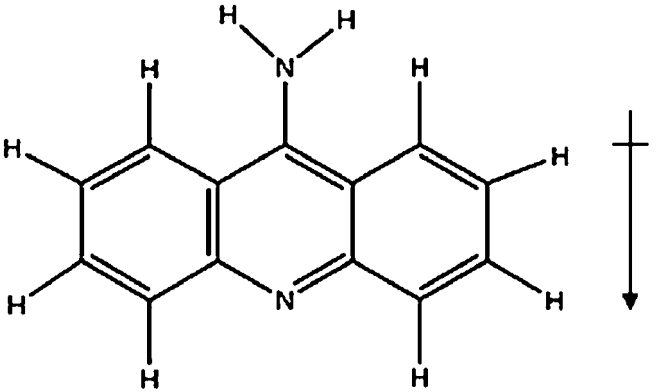

9-acridinamine (amino tautomer)

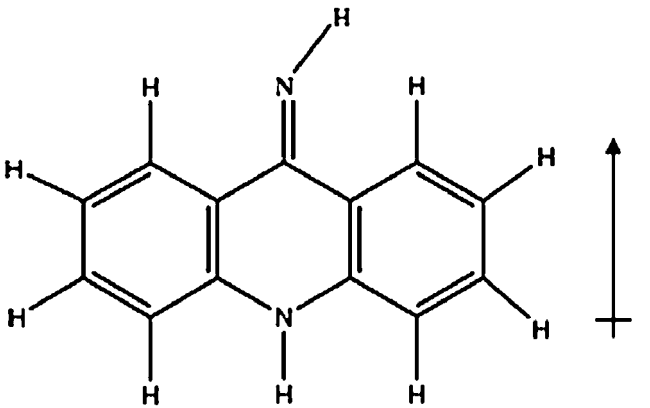

9-acridinamine (imino tautomer)

Figure 9 Chemical structures of the amino and imino tautomers of 9-acridinamine. The arrow indicates the direction of the dipole.

10. $X^- \cdot (H_2O)_n$ COMPLEXES

IR spectroscopy and electronic structure calculations have provided important insights into the nature of the bonding in small $X^- \cdot (H_2O)_n$ clusters, where X^- corresponds to an anion such as Cl^-, O_2^-, or SO_2^- (172–175). Although these anions in their ground states are not dipole-bound species, they are relevant to this

review since upon photoexcitation they can form charge-transfer states in which the electron is dipole bound. A classic example is $I^- \cdot (H_2O)_4$. In the most stable form of the ground state of this ion, the $(H_2O)_4$ entity has a crown-like structure with the four free OH groups pointed toward the I^- ion (50, 51). The resulting distorted water tetramer has a large dipole moment ($\mu \approx 3.65$D), which permits formation of the dipole-bound anion upon photoexcitation. Much of the recent interest in the $I^- \cdot (H_2O)_n$ clusters has focused on the evolution of the cluster following the initial charge-transfer event. Based on the results of femosecond photoelectron spectra, Lehr et al. have concluded that the charge-transfer excited state of $I^-(H_2O)_4$ rapidly distorts to a structure in which the excess electron autoionizes. For the larger $I^- \cdot (H_2O)_6$ species, there is evidence of isomerization in the 200 fsec timescale (57, 82). Several theoretical studies of the charge-transfer-to-solvent (CTTS) excited states of $I^- \cdot (H_2O)_n$ clusters, in particular, $I^- \cdot (H_2O)_4$, have been published recently (48–53). Because of the additional complexities presented by excited states and by the presence of the I atom, none of these studies has included high-order electron correlation effects.

11. POLARIZATION-BOUND STATES

Another class of weakly bound anions are those for which the excess electron is bound entirely, or predominately, as a result of electronic polarization rather than by the electrostatic field associated with the permanent charge distribution of the molecule or cluster of interest. Metal surfaces (176, 177) and certain metal (178) and inert-gas clusters (179–181), for example, Au_6 (178) and Xe_m, $m \geq 6$, (179, 182, 183) possess weakly bound surface states where the electron binding is dominated by polarization. In the case of Au_6, the polarization-bound anion is an electronically excited state of the cluster. These anions are relevant to the present review in that one can envision systems in which both polarization-bound and dipole- or other electrostatically bound anion states exist, and, perhaps, can interconvert. For example, for sufficiently large m, $(H_2O)_3Xe_m$ clusters with the water trimer on the surface, should possess both dipole-bound and polarization-bound anion states. There is also the interesting problem of the binding of an excess electron to systems in which neither the dipole moment nor the polarizability alone suffices to bind the electron, but which together results in electron binding. This problem has been explored to some extent by Abdoul-Carime and coworkers, using a one-electron model potential approach (184). However, the model used by these authors and those used by other researchers (181, 185) investigating binding of an electron by polarization alone did not allow for dispersion interactions. One-electron models employing quantum Drude oscillators to describe both polarization and dispersion would be ideally suited for addressing these issues.

It is also possible to envision systems in which the electron-binding is dispersion dominated. Indeed, Skurski et al. (165) have suggested that the amino-tautomer of 9-acridinamine should be viewed as being dispersion bound.

12. CONCLUSIONS

In this review we have focused on recent theoretical work on dipole-bound anions and the closely related solvated-electron species. Particular emphasis has been placed on elucidating the role of electron correlation effects, especially dispersion-type interactions in describing the binding of an excess electron. Dispersion-type interactions make large contributions to the electron binding in both dipole-bound and solvated-electron anions. This is an important observation because, until very recently, all one-electron models introduced to treat excess electrons interacting with water and other polar molecules, have neglected dispersion-type interactions. It is demonstrated that these interactions can be quantitatively described within a one-electron framework by the use of quantum Drude oscillators. The Drude model approach results in a huge reduction of computer time compared with traditional ab initio electronic structure methods. For example, for $(H_2O)_{12}^-$, a single-point Drude model calculation using the CI method requires only 20 seconds of CPU time on a Pentium IV PC, whereas an ab initio CCSD(T) calculation on this anion, described by a flexible basis set, would take several weeks of CPU time.

The importance of dispersion effects in the binding of excess electrons as dipole-bound or solvated-electron anions is sometimes "masked" in ab initio treatments because charge renormalization effects often act so as to make the electrostatic potential less attractive for the excess electron and thus to decrease electron binding. Higher-order electron correlation effects can also significantly impact electron binding energies and can cause a significant contraction of the charge distribution of the excess electron, which has important implications for vibrational spectroscopy of dipole-bound and solvated-electron species.

The need to include high-order correlation effects, e.g., by means of the CCSD(T) procedure, greatly restricts the size system for which accurate vibrational spectra can be calculated, which is, for example, a significant handicap in making definitive assignments of the isomers responsible for the observed $(H_2O)_6^-$ IR spectra. The new generation of model potentials employing Drude oscillators has the potential of solving this problem, but first it will be necessary to remove the constraint of rigid water monomers and to derive expressions for analytical gradients. The computational speed of the one-electron Drude model approach should permit coupling with approaches such as the vibrational SCF method (186), which would allow for inclusion of anharmonicity effects in calculation of the spectra.

ACKNOWLEDGMENTS

We acknowledge the support of the National Science Foundation and the Department of Energy for their support of our research in the area of electrons interacting with polar molecules. We especially want to acknowledge our collaborators Drs. J. Simons, M. Gutowski, M. Johnson, and F. Vila for many valuable discussions on weakly bound electron systems.

The *Annual Review of Physical Chemistry* is online at http://physchem.annualreviews.org

LITERATURE CITED

1. Fermi E, Teller E. 1947. *Phys. Rev.* 72:399
2. Wallis RF, Hermans R, Milnes HW. 1960. *J. Mol. Spectrosc.* 4:51
3. Crawford OH. 1967. *Proc. R. Soc. London* 91:279
4. Crawford OH, Dalgarno A. 1967. *Chem. Phys. Lett.* 1:23
5. Brown WB, Roberts RE. 1967. *J. Chem. Phys.* 46:2006
6. Turner JE, Anderson VE, Fox K. 1968. *Phys. Rev.* 174:81
7. Garrett WR. 1971. *Phys. Rev. A* 3:961
8. Garrett WR. 1980. *J. Chem. Phys.* 73:5721
9. Garrett WR. 1982. *J. Chem. Phys.* 77: 3666
10. Griffing KM, Kenney J, Simons J, Jordan KD. 1975. *J. Chem. Phys.* 63:4073–75
11. Jordan KD, Luken W. 1976. *J. Chem. Phys.* 64:2760–66
12. Jordan KD, Wendoloski J. 1977. *Chem. Phys.* 21:145–54
13. Jordan KD, Wendoloski J. 1978. *Mol. Phys.* 35:223–40
14. Shortley GH. 1931. *Phys. Rev.* 38:120–27
15. Laudau LD, Lifshitz EM. 1959. Motion in a centrally symmetric field. In *Quantum Mechanics*, pp. 118–21. Oxford: Pergamon
16. Born M, Oppenheimer R. 1927. *Ann. Phys.* 84:457
17. Crawford OH. 1968. *Chem. Phys. Lett.* 2:461
18. Garrett WR. 1970. *Chem. Phys. Lett.* 5:393
19. Clary DC. 1988. *J. Phys. Chem.* 92:3173
20. Jordan KD. 1979. *Acc. Chem. Res.* 12:36
21. Simons J, Jordan KD. 1987. *Chem. Rev.* 87:535
22. Gutowski M, Skurski P, Boldyrev AI, Simons J, Jordan KD. 1996. *Phys. Rev. A* 54:1906
23. Gutowski M, Jordan KD, Skurski P. 1998. *J. Phys. Chem. A* 102:2624
24. Yokoyama K, Leach GW, Kim JB, Lineberger WC, Boldyrev AI, Gutowski M. 1996. *J. Chem. Phys.* 105:10706
25. Gutowski M, Skurski P. 1999. *Recent Res. Dev. Phys. Chem.* 3:245
26. Gutowski M, Skurski P. 1999. *Chem. Phys. Lett.* 300:331
27. Adamowicz L. 1989. *J. Chem. Phys.* 91:7787–90
28. Adamowicz L, McCullough EA. 1984. *J. Phys. Chem.* 88:2045
29. Desfrancois C, Periquet V, Carles S, Schermann JP, Smith DMA, Adamowicz L. 1999. *J. Chem. Phys.* 110:4309–14
30. Pople JA, Head-Gordon M, Raghavachari K. 1987. *J. Chem. Phys.* 87:5968
31. Peterson KA, Gutowski M. 2002. *J. Chem. Phys.* 116:3297
32. Wang F, Jordan KD. 2001. *J. Chem. Phys.* 114:10717–24
33. Wang F, Jordan KD. 2002. *J. Chem. Phys.* 116:6973–81
34. Sindelka M, Spirko V, Jungwirth P. 2002. *J. Chem. Phys.* 117:5113
35. Compton RN, Carman HS Jr, Desfrancois C, Abdoul-Carime H, Schermann JP, et al. 1996. *J. Chem. Phys.* 105:3472
36. Desfrancois C, Periquet V, Lyapustina SA, Lippa TP, Robinson DW, Bowen KH. 1999. *J. Chem. Phys.* 111:4569–76
37. Lecomte F, Carles S, Desfrancois C, Johnson MA. 2000. *J. Chem. Phys.* 113:10973
38. Smith DMA, Smets J, Adamowicz L. 1999. *J. Phys. Chem. A* 103:4309–12
39. Smith DMA, Smets J, Adamowicz L. 1999. *J. Phys. Chem. A* 103:5784–90
40. Hall CS, Adamowicz L. 2002. *J. Phys. Chem. A* 106:6099–101
41. Jalbout AF, Smets J, Adamowicz L. 2001. *Chem. Phys.* 273:51–58

42. Hendricks JH, Lyapustina SA, de Clercq HL, Snodgrass JT, Bowen KH. 1996. *J. Chem. Phys.* 104:7788
43. Skurski P, Simons J. 2001. *J. Chem. Phys.* 115:8373
44. Desfrancois C, Carles S, Schermann JP. 2000. *Chem. Rev.* 100:3943–62
45. Rak J, Skurski P, Gutowski M. 2001. *J. Chem. Phys.* 114:10673
46. Gutowski M, Skurski P, Simons J. 2000. *J. Am. Chem. Soc.* 122:10159
47. Skurski P, Gutowski M, Barrios R, Simons J. 2001. *Chem. Phys. Lett.* 337:143
48. Davis AV, Zanni MT, Frischkorn C, Neumark DM. 2000. *J. Electron Spectrosc.* 108:203
49. Majumdar D, Kim J, Kim KS. 2000. *J. Chem. Phys.* 112:101–5
50. Serxner D, Sessent CE, Johnson MA. 1996. *J. Chem. Phys.* 105:7231
51. Vila F, Jordan KD. 2002. *J. Phys. Chem. A* 106:1391–97
52. Chen H-Y, Sheu W-S. 2000. *J. Am. Chem. Soc.* 122:7534
53. Chen H-Y, Sheu W-S. 2001. *Chem. Phys. Lett.* 335:475
54. Guthe F, Tulej M, Mickhail T, Pachkov V, Maier JP. 2001. *Astrophys. J.* 555:466–71
55. Ayotte P, Bailey CG, Kim J, Johnson MA. 1998. *J. Chem. Phys.* 108:444–49
56. Ayotte P, Weddle GH, Bailey CG, Johnson MA, Vila F, Jordan KD. 1999. *J. Chem. Phys.* 110:6268–77
57. Lehr L, Zanni MT, Frischkorn C, Weinkauf R, Neumark DM. 1999. *Science* 284:635
58. Desfrancois C, Abdoul-Carime H, Khelifa N, Schermann JP. 1994. *Phys. Rev. Lett.* 73:2436
59. Compton RN, Hammer NI. 2001. Multiple-bound molecular anions. In *Advances in Gas-Phase Ion Chemstry*, ed. NG Adams, pp. 257–305. Greenwich,CT: JAI
60. Desfrancois C. 1995. *Phys. Rev. A* 51: 3667
61. Power JD. 1974. *Philos. Trans. R. Soc. London A* 274:663
62. Moiseiwitsch BL. 1961. *Quantum Theory*. New York: Academic
63. Garrett WR. 1979. *J. Chem. Phys.* 71:651
64. Koopmans T. 1934. *Physica (Amsterdam)* 1:104
65. Gutowski M, Skurski P, Jordan KD, Simons J. 1997. *Int. J. Quantum Chem.* 64:183
66. Gutsev GL, Bartlett RJ. 1996. *J. Chem. Phys.* 105:8785
67. Gutowski M, Skurski P. 1997. *J. Phys. Chem. B* 101:9143
68. Jalbout AF, Adamowicz L. 2001. *J. Phys. Chem. A* 105:1033–38
69. Jalbout AF, Hall-Black CS, Adamowicz L. 2002. *Chem. Phys. Lett.* 354:128–33
70. Schiedt J, Weinkauf R, Neumark DM, Schlag EW. 1998. *Chem. Phys.* 239:511
71. Laenen R, Roth T, Laubereau A. 2000. *Phys. Rev. Lett.* 85:50
72. Silva C, Walhout PK, Yokoyama K, Barbara PF. 1998. *Phys. Rev. Lett.* 80:1086
73. Bartels DM, Cook AR, Mudaliar M, Jonah CD. 2000. *J. Phys. Chem. A* 104:1686–91
74. Crowell RA, Bartels DM. 1996. *J. Phys. Chem.* 100:17713–15
75. Bartels DM, Gosztola D, Jonah CD. 2001. *J. Phys. Chem. A* 105:8069
76. Coe JV. 2001. *Int. Rev. Phys. Chem.* 20:33–58
77. Tauber MJ, Mathies RA. 2002. *Chem. Phys. Lett.* 354:518–26
78. Staib A, Borgis D. 1996. *J. Chem. Phys.* 104:9027
79. Sheu W, Rossky PJ. 1993. *Chem. Phys. Lett.* 213:233
80. Long FH, Shi H, Lu K, Eisenthal B. 1994. *J. Chem. Phys.* 98:7252
81. Gaudeul Y, Gelabert H, Ashokkumar M. 1995. *Chem. Phys.* 197:167
82. Kloepfer JA, Vilchiz VH, Lenchenkov VA, Bradforth SE. 1998. *Chem. Phys. Lett.* 298:120
83. Sobolewski AL, Domcke W. 2002. *Phys. Chem. Chem. Phys.* 4:4–10
84. Muguet FF, Gelabert H, Gaudeul Y. 1996. *J. Chem. Phys.* 93:1808

85. Tuttle TR Jr, Golden S. 1991. *J. Phys. Chem.* 95:5725
86. Hart EJ, Anbar M. 1970. *The Hydrated Electron*. New York: Wiley-Intersci.
87. Kevan L. 1981. *Acc. Chem. Res.* 14
88. Schnitker J, Rossky PJ. 1987. *J. Chem. Phys.* 86:3471
89. Ayotte P, Johnson MA. 1997. *J. Chem. Phys.* 106:811–14
90. Tauber MJ, Mathies RA. 2001. *J. Phys. Chem. A* 105:10952
91. Haberland H, Ludewigt C, Shindler H, Worsnop R. 1985. *Z. Phys. A* 320:151
92. Wallqvist A, Thirumalai D, Berne BJ. 1986. *J. Chem. Phys.* 85:1583
93. Boutellier Y, Desfrancois C, Abdoul-Carime H, Schermann JP. 1996. *J. Chem. Phys.* 105:6420
94. Kim KS, Park I, Lee S, Cho K, Lee JY, et al. 1996. *Phys. Rev. Lett.* 76:956
95. Coe JV. 1997. *J. Phys. Chem. A* 101:2055–63
96. Maeyama T, Tsumura T, Fujii A, Mikami N. 1997. *Chem. Phys. Lett.* 264:292
97. Kim J, Becker I, Cheshnovsky O, Johnson MA. 1998. *Chem. Phys. Lett.* 297:90–96
98. Smith DMA, Smets J, Elkadi Y, Adamowicz L. 1998. *J. Chem. Phys.* 109:1238
99. Novakovskaya YV, Stepanov NF. 2002. *Int. J. Quantum Chem.* 88:496–506
100. Haberland H, Schindler HG, Worsnop R, Bunsenges B. 1984. *Phys. Chem.* 88:271
101. Lee HM, Suh SB, Lee JY, Tarakeshwar P, Kim KS. 2000. *J. Chem. Phys.* 112:9759
102. Lee HM, Suh SB, Lee JY, Tarakeshwar P, Kim KS. 2001. *J. Chem. Phys.* 114:3343
103. Lee HM, Suh SB, Kim KS. 2001. *J. Chem. Phys.* 114:10749–56
104. Suh SB, Lee HM, Kim J, Lee JY, Kim KS. 2000. *J. Chem. Phys.* 113:5273–77
105. Smith DMA, Smets J, Adamowicz L. 1999. *J. Chem. Phys.* 110:3804–10
106. Lee HM, Suh SB, Kim KS. 2000. *Bull. Kor. Chem. Soc.* 21:555–56
107. Bailey CG, Kim J, Johnson MA. 1996. *J. Phys. Chem.* 100:16782
108. Becke AD. 1993. *J. Chem. Phys.* 98:5648
109. Mielich B, Savin A, Stoll H, Preuss H. 1989. *Chem. Phys. Lett.* 157:200
110. Lee C, Yang W, Parr RG. 1988. *Phys. Rev. B* 37:785–89
111. Elstner M, Hobza P, Frauenheim T, Suhai S, Kaxiras E. 2001. *J. Chem. Phys.* 114:5149
112. Rigby M, Smith EB, Wakeham WA, Maitland GC. 1986. *The Forces Between Molecules*. Oxford: Clarendon
113. Cao J, Berne BJ. 1992. *J. Chem. Phys.* 97:8628
114. Barnett RN, Landman U, Cleveland CL, Jortner J. 1988. *J. Chem. Phys.* 88:4421
115. Schnitker J, Rossky PJ. 1987. *J. Chem. Phys.* 86:3462
116. Staib A, Borgis D. 1995. *J. Chem. Phys.* 103:2642
117. Mosyak A, Graf P, Benjamin I, Nitzan A. 1996. *J. Phys. Chem. A* 101:429
118. Barnett RN, Landman U, Scharf D, Jortner J. 1989. *Acc. Chem. Res.* 22:350
119. Marchi M, Sprik M, Klein ML. 1988. *J. Chem. Phys.* 89:4918
120. Landman U, Barnett RN, Cleveland CL, Luo J, Scharf D, Jortner J. 1987. Simulations of structures, dynamics, and transformations in finite aggregates. In *Few Body Systems and Multiparticle Dynamics*, ed. D Micha, p. 200. New York: AIP
121. Benjamin I, Evans D, Nitzan A. 1997. *J. Chem. Phys.* 106:6647
122. Barnett RN, Landman U, Nitzan A. 1988. *J. Chem. Phys.* 89:2242
123. Barnett RN, Landman U, Nitzan A. 1989. *Phys. Rev. Lett.* 62:106
124. Dang LX, Chang TM. 1997. *J. Chem. Phys.* 106:8149
125. Pedulla JM, Jordan KD. 1998. *Chem. Phys.* 239:593
126. Verhoeven J, Dymanus A. 1970. *J. Chem. Phys.* 52:3222
127. Shepard AC, Beers Y, Klein GP, Rothman LS. 1973. *J. Chem. Phys.* 59:2254
128. Stillinger FH. 1982. Low frequency dielectric properties of liquid and solid water. In *The Liquid State of Matter; Fluids, Simple and Complex*, ed. EW Montroll,

JL Lebowitz, p. 341. Amsterdam: North-Holland
129. Skurski P, Gutowski M, Simons J. 2000. *Int. J. Quantum Chem.* 80:1024–38
130. Alfonso DR, Jordan KD. 2002. *J. Chem. Phys.* 116:3612–16
131. Deleted in Proof
132. Deleted in Proof
133. Abdoul-Carime H, Schermann JP, Desfrancois C. 2002. *Few-Body Systems* 31:183–90
134. Mullin AS, Murray KK, Schulz CP, Lineberger WC. 1993. *J. Phys. Chem.* 97:10281–86
135. Coe JV, Lee GH, Eaton JG, Arnold ST, Sarkas HW, et al. 1990. *J. Chem. Phys.* 92:3980
136. Novick SE, Jones PL, Mulloney TJ, Lineberger WC. 1979. *J. Chem. Phys.* 70:2210–14
137. Gutowski M, Hall CS, Adamowicz L, Hendricks JH, de Clercq HL, et al. 2002. *Phys. Rev. Lett.* 88:143001
138. Sunil KK, Jordan KD. 1989. *Chem. Phys. Lett.* 164:509
139. Skurski P, Simons J. 2002. *J. Chem. Phys.* 116:6118–25
140. Skurski P, Gutowski M, Simons J. 2000. *Chem. Phys. Lett.* 322:175
141. Gutowski M, Skurski P, Simons J. 2000. *Int. J. Mass Spectrom.* 201:245
142. Ambika Prasad MVN, Wallis RF, Hermans R. 1989. *Phys. Rev. B* 40:5924
143. Jordan KD, Liebman JF. 1979. *Chem. Phys. Lett.* 62:143
144. Gutowski M, Skurski P. 1999. *Chem. Phys. Lett.* 303:65
145. Ambika Prasad MVN, Wallis RF, Hermans J. 1991. *Solid State Commun.* 77:973
146. Simons J, Skurski P. 2002. The roles of electrostatics in forming molecular anions and dianions. In *Theoretical Prospects of Negative Ions*, ed. J Kalcher, pp. 117–38. Trivandrum: Research Signpost
147. Gutsev GL, Bartlett RJ, Compton RN. 1998. *J. Chem. Phys.* 108:6756
148. Halamaries A, Walker CW, Simth KA, Dunning FB. 1988. *J. Chem. Phys.* 89
149. Harth K, Ruf MW, Hotop HZ. 1989. *Z. Phys. D* 14:149
150. Jordan KD, Burrow PD. 1978. *Acc. Chem. Res.* 11:341–48
151. Desfrancois C, Periquet V, Carles S, Schermann JP, Adamowicz L. 1998. *Chem. Phys.* 239:475–83
152. Desfrancois C, Abdoul-Carime H, Schermann JP. 1996. *J. Chem. Phys.* 104
153. Lykke KR, Mead RD, Lineberger WC. 1984. *Phys. Rev. Lett.* 52:2221
154. Wetzel D, Brauman JI. 1989. *J. Chem. Phys.* 90:68
155. Nelson RD, Lide DR, Margott AA. 1967. *Selected Values of Electric Dipole Moments for Molecules in Gas Phase*. Washington, DC: Natl. Bur. Stand.
156. Gutsev GL, Bartlett RJ. 1996. *J. Chem. Phys.* 105:8785–92
157. Modelli A, Venuti M. 2001. *Int. J. Mass Spectrom.* 205:7–16
158. Sommerfeld T. 2002. *Phys. Chem. Chem. Phys.* 4:2511
159. Desfrancois C, Periquet V, Boutellier Y, Schermann JP. 1998. *J. Phys. Chem. A* 102:1274–78
160. Hendricks JH, Lyapustina SA, de Clercq HL, Bowen KH. 1998. *J. Chem. Phys.* 108:8–11
161. Aflatooni K, Gallup GA, Burrow PD. 1998. *J. Phys. Chem.* 102:6205–7
162. Sevilla MD, Besler B, Colson AO. 1995. *J. Phys. Chem.* 99:1060
163. Hendricks JH, Lyapustina SA, de Clercq HL, Bowen KH. 1997. *J. Chem. Phys.* 108:8–11
164. Sevilla MD, Besler B, Colson AO. 1994. *J. Chem. Phys.* 98:2215
165. Skurski P, Rak J, Simons J. 2001. *J. Chem. Phys.* 115:11193–99
166. Rak J, Blazejowski J, Zauhar RJ. 1992. *J. Organomet. Chem.* 57
167. Jungwirth P, Spirko V. 2000. *Phys. Rev. Lett.* 84:1140
168. Skurski P, Gutowski M, Simons J. 1998. *Int. J. Quantum Chem.* 76:197

169. Sarasola C, Fowler JE, Ugalde JM. 1999. *J. Chem. Phys.* 110:11717
170. Sarasola C, Fowler JE, Elorza JM, Ugalde JM. 2001. *Chem. Phys. Lett.* 337: 355
171. Skurski P, Simons J. 2000. *J. Chem. Phys.* 112:6563
172. Woronowic EA, Robertson WH, Weddle GH, Myshakin EM, Jordan KD, Johnson MA. 2002. *J. Phys. Chem. A* 106:7086–89
173. Weber JA, Kelly WH, Robertson MA, Johnson MA. 2001. *J. Chem. Phys.* 114:2698–706
174. Myshakin EM, Robertson WH, Weddle GH, Jordan KD, Johnson MA. 2003. *J. Chem. Phys.* In press
175. Cabarcos OM, Weinheimer CJ, Lisy JM, Xantheas SS. 1999. *J. Chem. Phys.* 110:5–8
176. Schoenlein RW, Fujimoto JG, Eesley GL, Capehat TW. 1988. *Phys. Rev. Lett.* 61:2596
177. Echenique PM, Pendry JB. 1989. *Prog. Surf. Sci.* 32:111
178. Taylor KJ, Jin C, Conceicao J, Wang L, Cheshnovsky O, et al. 1990. *J. Chem. Phys.* 93:7515
179. Martyna CJ, Berne BJ. 1989. *J. Chem. Phys.* 90:3744
180. Haberland H, Bowen KH. 1994. Solvated electron clusters. In *Clusters of Atoms and Molecules II. Solvation and Chemistry of Free Clusters and Embedded, Supported and Compressed Clusters*, ed. H Haberland, pp. 134. Berlin: Springer
181. Stampfli P, Bennemann K. 1988. *Phys. Rev. A* 38:4431
182. Haberland H, Kolar T, Reiners T. 1989. *Phys. Rev. Lett.* 63:1219
183. Martyna CJ, Berne BJ. 1988. *J. Chem. Phys.* 88:4516
184. Abdoul-Carime H, Desfrancois C. 1998. *Eur. Phys. J. D* 2:149–56
185. Rosenblit M, Jortner J. 1994. *J. Phys. Chem.* 98:9365–70
186. Jung JO, Gerber RB. 1996. *J. Chem. Phys.* 105:10322
187. Gutowski M, Skurski P. 1997. *J. Chem. Phys.* 107:2968
188. Skurski P, Gutowski M. 1998. *J. Chem. Phys.* 108:6303
189. Arnold ST, Eaton JG, Patel-Misra D, Sarkas HW, Bowen KH. 1989. *Ion and Cluster Ion Spectroscopy and Structure*. Amsterdam: Elsevier
190. Boutellier Y, Desfrancois C, Abdoul-Carime H, Schermann JP. 1996. *J. Chem. Phys.* 105:6420
191. Hendricks JH, de Clercq HL, Lyapustina SA, Bowen KH. 1997. *J. Chem. Phys.* 107:2962
192. Berendsen HJC, Postma JPM, Van Gunsteren WF, Hermans J. 1981. Interaction models for water in relation to protein hydration. In *Intermolecular Forces*, ed. B Pullman, p. 331. Dordrecht: Reidel
193. Reimers JR, Watts RO. 1984. *Chem. Phys.* 85:83
194. Sprik M, Klein ML. 1988. *J. Chem. Phys.* 89:7556
195. Lemberg HL, Stillinger FH. 1975. *J. Chem. Phys.* 62:1677
196. Dang LX. 1992. *J. Chem. Phys.* 97: 2659

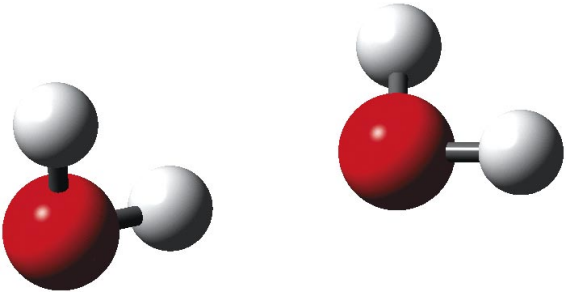

Figure 4 Geometry of $(H_2O)_2^-$ used to determine the repulsive core scaling parameter and the cutoff parameter in the Drude model.

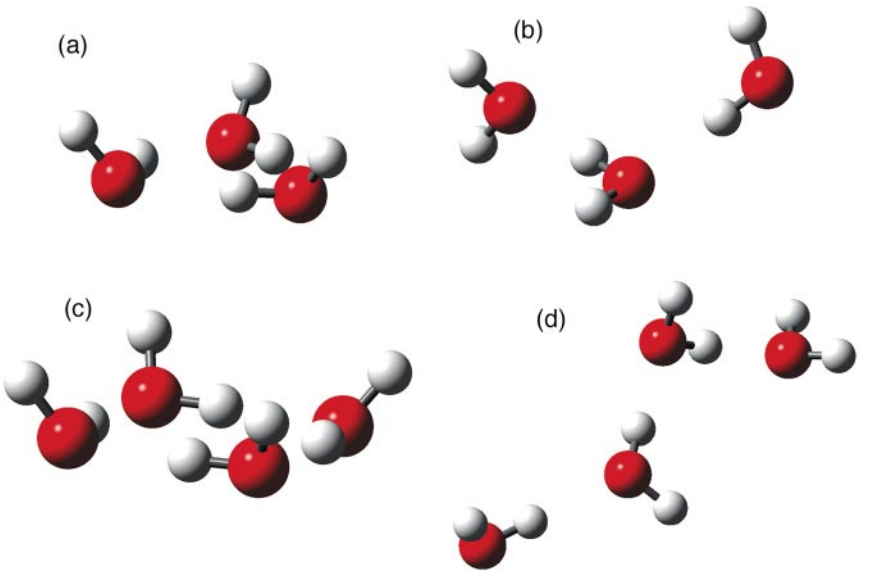

Figure 5 The geometries of crown (*a*) and linear (*b*) forms of $(H_2O)_3^-$ and crown (*c*) and linear (*d*) forms of $(H_2O)_4^-$.

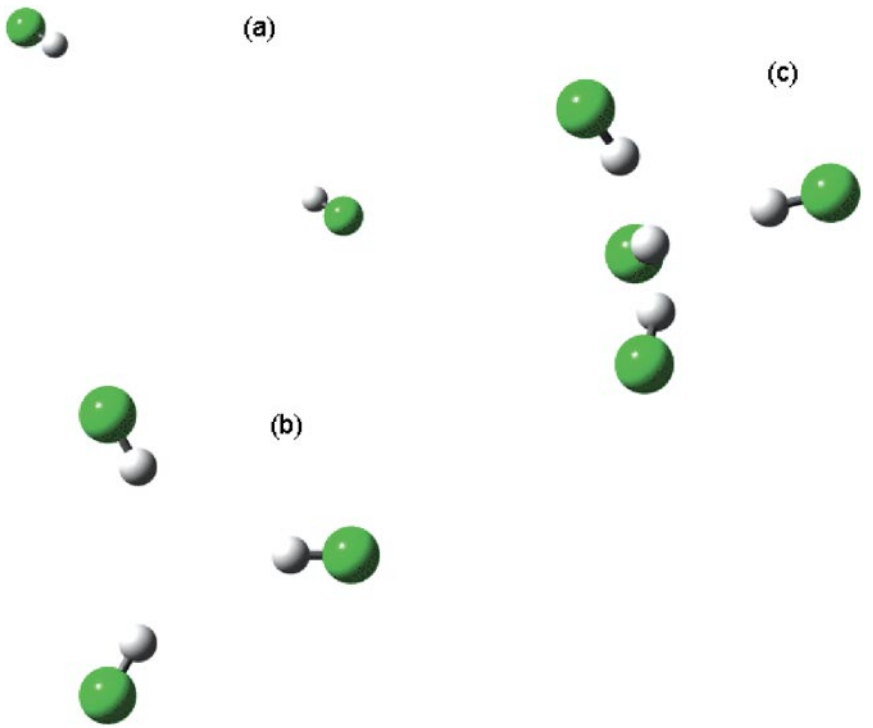

Figure 7 Arrangements of $(HF)_n$, $n = 2$–4, with overall net dipole moments of zero. (*a*) $n = 2$, (*b*) $n = 3$, (*c*) $n = 4$.

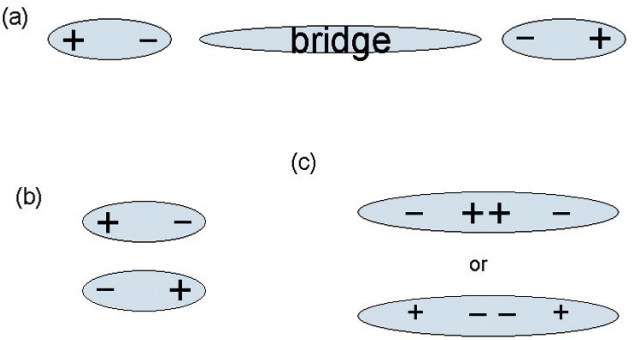

Figure 8 Schematic charge arrangements that can give bi-dipole-bound anion (*a*) and quadrupole bound anion (*b*) and (*c*).